Efficient Transmission over Unknown Channels

RANJITHA GUBBI SURESH
MASTER´S THESIS
DEPARTMENT OF ELECTRICAL AND INFORMATION TECHNOLOGY
FACULTY OF ENGINEERING | LTH | LUND UNIVERSITY

Efficient Transmission over Unknown Channels

Ranjitha Gubbi Suresh
ra1265gu-s@student.lu.se

Department of Electrical and Information Technology
Lund University

Supervisors: Michael Lentmaier, Saeedeh Moloudi and
Leif Wilhelmsson

Examiner: Fredrik Rusek

June 14, 2020

Printed in Sweden
Tryckeriet i E-huset, Lund

Abstract

In recent years, digital transmission techniques have been continuously evolving by employing increasingly more advanced Modulation and Coding Scheme (MCS). However, when the wireless channel is varying rapidly, it is hard or even impossible for the transmitter to select the proper MCS.

In this thesis work, a high MCS is employed at the transmitter, irrespective of channel conditions, in order to exploit the channel in an opportunistic way. A detailed description of Multi-Layer Transmission (MLT) using high MCS in combination with Hybrid Automatic Repeat reQuest (HARQ) scheme is presented, and its performance is compared with the traditional transmission technique with the aid of Matlab simulations. The thesis illustrates the gain in the performance of mixing layers in MLT and also outlines the idea of employing successive demodulation at the receiver side. Furthermore, the performance of MLT with the basic ARQ scheme is also investigated in this thesis work.

Keywords: Multi-Layer Transmission, RBIR, HARQ, mixing layers, successive demodulation, Wi-Fi

Acknowledgements

I would like to express my gratitude to my supervisors Leif Wilhelmsson and Saeedeh Moloudi, for the guidance through each stage of the thesis. I'm very grateful for their insightful feedback, discussions, and suggestions that have helped me expand my horizon. It was fantastic working with them, and I thoroughly enjoyed my journey at Ericsson.

Also, I would like to thank my university supervisor Michael Lentmaier for his constant support throughout my master's studies. I'm incredibly thankful for all the sincere and valuable guidance and encouragement extended to me.

Finally, I would like to express my gratitude to my parents and my friends for providing me with all the support and encouragement throughout my studies.

Table of Contents

List of Figures

List of Tables

List of Acronyms

ARQ	Automatic Repeat reQuest
AWGN	Additive White Gaussian Noise
BICM	Bit-Interleaved Coded Modulation
BLER	BLock Error Probability
CM	Coded Modulation
CSI	Channel State Information
FEC	Forward Error Correction
HARQ	Hybrid Automatic Repeat reQuest
IID	Independent and Identically Distributed
LA	Link Adaptation
LDPC	Low Density Parity Check
LLR	Log-Likelihood Ratio
MCS	Modulation and Coding Scheme
MLCM	Multi-Layer Coded Modulation
MLT	Multi-Layer Transmission
QAM	Quadrature Amplitude Modulation
RBIR	Received Bit Information Rate
SI	Symbol-level mutual Information
SINR	Signal-to-Interference-plus-Noise Ratio
SNR	Signal-to-Noise Ratio

Chapter 1

Introduction

Digital transmission techniques play a vital role in the design of communication systems. They basically aim to provide an error-free reconstruction of the original information at the receiver despite the variations in channel conditions, thereby improving the reliability of the communication link. To achieve this, a proper Modulation and Coding Scheme (MCS) must be selected based on the Channel State Information (CSI) available at the moment of every transmission and the technique used to realize this is often known as Link Adaptation (LA). However, when the channel is changing fast, LA is a main challenge to achieve reliable communication over wireless networks.

When wireless communication takes place in an unlicensed spectrum, which is the case for Wi-Fi or Bluetooth, the channel conditions may vary considerably due to the variations in the experienced interference from other devices. These variations make it hard, or even impossible, for the transmitter to select the proper MCS. In these cases, LA cannot work properly because the channel is varying very fast, i.e., the channel information gets outdated very quickly. In this thesis work, the idea is to exploit the channel opportunistically by employing a high MCS at the transmitter irrespective of channel conditions using Multi-Layer Transmission (MLT) with Hybrid Automatic Repeat reQuest (HARQ) scheme.

The approach and methodology of this thesis work are based on the close relationship between understanding the theoretical foundation, based on the work by Shannon [1], and the performance of a practical communication system employing multi-layer transmission intended to a single user, based on the coding and modulation used in IEEE 802.11, i.e., Wi-Fi. It is assumed that the channel conditions are largely unknown to the transmitter.

1.1 Goal of the Project

In this work, the concepts of Received Bit Information Rate (RBIR) will be used to analyze the performance of MLT in combination with the HARQ-CC (Chase Combining) scheme with respect to the traditional approach, where the codewords are sent serially one after the other. Furthermore, different variants of MLT and their performances are compared to the standard multi-layer approach. Firstly, the

mixing of layers during retransmission of unsuccessful-decoded codewords will be studied with respect to the standard multi-layer approach to understand how the suitable selection of layer for retransmission further influences the performance. Secondly, the idea of employing successive demodulation in MLT will be investigated, and its performance will be compared with the parallel demodulation technique (i.e., independent demodulation). Lastly, MLT with the basic Automatic Repeat reQuest (ARQ) scheme will be investigated.

The goal of the thesis work is to understand under what conditions MLT performs better than the traditional approach and also to investigate how the performance of a standard multi-layer approach can be further improved by properly choosing the system parameters.

1.2 Related Work

Multi-layer transmission techniques are often used in broadcast applications where there is no feedback response from the intended users. However, these applications demand strong error-correcting codes such that the reliability is not compromised. On the other hand, in the paper [2], the multi-layer broadcast approach was analysed in combination with the HARQ scheme in order to improve the performance when different receivers were subjected to different channel conditions.

In dense environments (e.g., unlicensed bands), LA at the transmitter cannot work properly as the channel is varying fast and the CSI gets outdated very quickly. In papers [3] [4], this issue was addressed by using the MLT in combination with the HARQ scheme for the next generation Wi-Fi standards. The results show that the MLT approach outperforms the traditional transmission approach when the channel is varying fast, thereby removing the need for link adaptation. Inspired by the performance of MLT approach, this thesis focuses on how the choice of various parameters further impacts the performance of MLT.

1.3 Thesis Outline

The outline of this thesis work is as follows; Chapter 2 introduces the basic concepts for understanding this thesis. The theoretical concepts of RBIR and its relation to different HARQ schemes are described in Chapter 3. Following, Chapter 4 introduces the structure, operation, and performance of the MLT. Further performance improvements using different variants of the multi-layer approach are outlined in Chapter 5. Finally, the conclusion and future work are summarized in Chapter 6.

Chapter 2
Background

Wireless communication systems often suffer from noise and interference on the channel, especially in dense deployments. To achieve reliable communication using these systems, the choice of system parameters plays an important role. This chapter briefly describes the underlying concepts in communication theory to understand how these system parameters can be selected and how they impact the performance of communication system.

2.1 Information Theory

Information theory is concerned with transmission rates that are required to transmit information from one point to another reliably. It also deals with the amount of information generated by a given source. As per this theory, the measure of information is related to its probability of occurrence but not on its actual content [5]. For instance, if a given source generates a message x from a set of possible messages X with the probability $p(x)$, then the measure of its information (i.e., self-information) is given by,

$$I(x) = -\log_2[p(x)]. \tag{2.1}$$

2.1.1 Entropy

The entropy of a random variable is defined as a measure of average uncertainty in that random variable. It can also be defined as the average value of $I(x)$ and is given by

$$H(X) = -\sum_{x} p(x)\log_2[p(x)]. \tag{2.2}$$

Likewise, the conditional entropy of a random variable X given a random variable Y is given by

$$H(X|Y) = -\sum_{x\epsilon X}\sum_{y\epsilon Y} p(x,y)\log_2[p(x|y)]. \tag{2.3}$$

where $p(x,y)$ is the joint probability of random variables X and Y and $p(x|y)$ is the conditional probability of X given Y.

2.1.2 Mutual Information

The average information of a random variable X obtained by observing a random variable Y is defined as the mutual information, and it is denoted by $I(X;Y)$ [5]. Mathematically, the mutual information between two random variables X and Y is given by

$$I(X;Y) = \sum_{x\epsilon X} \sum_{y\epsilon Y} p(x,y) \log_2 \left[\frac{p(x,y)}{p(x)p(y)} \right]. \tag{2.4}$$

It can also be described as the reduction in uncertainty of a random variable X by observing another random variable Y. The relation between them is as follows,

$$I(X;Y) = H(X) - H(X|Y). \tag{2.5}$$

Chain Rule for Mutual Information

For a set of random variables X_1, X_2, X_3,.....X_L, the information content of these variables given the random variable Y is defined by the chain rule of mutual information as follows,

$$I(X_1, X_2, ..., X_i; Y) = \sum_{i=1}^{L} I(X_i; Y|X_1, X_2, ...X_{i-1}). \tag{2.6}$$

2.2 Coding Theory

The information bits are often protected by adding redundant bits in a predefined way to correct channel errors during transmission. This process of adding redundancy is termed as channel encoding. At the receiver side, these redundant bits are used to extract the original information bits. The codes used for encoding and decoding are commonly known as Forward Error Correction (FEC) codes. One class of FEC codes that is widely used is a linear block code, which represents K-bit information $\boldsymbol{u}$ by using N-bit codeword $\boldsymbol{v}$, and its rate is defined by $r = K/N$. A linear block code is generally represented as (N, K) code. Each codeword is generated using a generator matrix G of size $K \times N$, i.e., $\boldsymbol{v} = \boldsymbol{u} \cdot G$.

A parity check matrix H_p of a linear block code is defined by a matrix of size $(N-K) \times N$ such that each codeword $\boldsymbol{v}$ satisfies the condition $\boldsymbol{v} \cdot H_p = 0$. In recent years, a class of linear block codes called Low Density Parity Check (LDPC) codes are used extensively in the wireless industry as their performance is very close to the Shannon limit.

2.2.1 Low Density Parity Check (LDPC) codes

An LDPC code is a linear block code characterized by a parity check matrix H_p that has relatively smaller number of ones when compared to zeros. The sparse characteristic of H_p allows various iterative decoding methods to provide near-capacity performance while the decoding complexity is not high [6]. An LDPC

code is said to be a regular code if the number of ones in a row (i.e. row weight w_r) and the number of ones in a column (i.e. column weight w_c) of H_p are same for all rows and columns respectively. If the row weight w_r and the column weight w_c of H_p are different, then they are said to be irregular LDPC codes. Throughout this thesis work, only binary irregular LDPC codes are considered.

Graphical Representation of LDPC codes

A Tanner graph is a bipartite graph whose nodes are decomposed into two sets such that every edge in a graph connects only the nodes belonging into different sets, and no two nodes of the same set are connected by an edge. The Tanner graph of an LDPC code provides a graphical representation of the H_p matrix of the code, and it helps in visualizing the decoding process. The two sets of nodes in Tanner graphs of LDPC codes are check nodes and variables nodes and are denoted by P and V, respectively, which corresponds to the number of check equations and number of code bits in H_p respectively [6].

For a given parity check matrix H_p of dimension $m \times n$, there are m check nodes and n variable nodes, where m and n denote the number of rows and columns of H_p, respectively. For each element h_{ij} of H_p equal to 1, an edge is connected between the i^{th} check node P_i and the j^{th} variable node V_j.

Example 2.1

$$H_p = \begin{bmatrix} 1 & 1 & 1 & 0 & 0 & 0 & 0 & 0 \\ 1 & 0 & 0 & 1 & 0 & 0 & 1 & 0 \\ 0 & 0 & 0 & 1 & 1 & 1 & 0 & 0 \\ 0 & 1 & 0 & 0 & 1 & 0 & 0 & 1 \end{bmatrix}$$

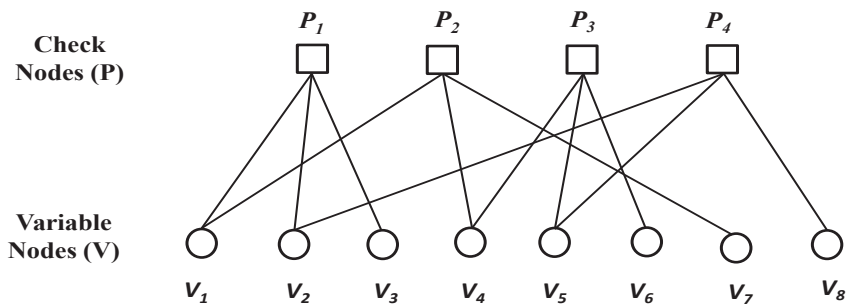

Figure 2.1: Illustration of Tanner Graph for parity check matrix H_p.

Consider a (8, 4) LDPC code with parity check matrix H_p as shown in Example 2.1. Since the row weight w_r and the column weight w_c are not constant, the parity check matrix H_p belongs to irregular LDPC code of rate $r = 0.5$. The corresponding Tanner graph is shown in Figure 2.1, where there are 4 check nodes $(P_1, P_2, \ldots, P_4)$ and 8 variable nodes $(V_1, V_2, \ldots, V_8)$ which are connected by edges for each element of H_p equal to 1.

Decoding Algorithms

The sparse characteristic of the parity check matrix allows iterative decoding of LDPC codes of reasonable complexity. For error rates of interest, these iterative decoding algorithms provide near-capacity performance. In a basic iterative algorithm, the received channel values (e.g., Log-Likelihood Ratio (LLR)) are fed to the variable nodes V of a Tanner graph. During the first stage of the iterative algorithm, the check nodes P take the inputs from their respective variable nodes and process them in a predefined way to send out the outputs to each of their respective variable nodes. In the second stage, these variable nodes take inputs from the channel and their respective check nodes, and after processing, they deliver the outputs to each of their respective check nodes. This process of exchanging information between the variable nodes V and the check nodes P is known as a message passing algorithm, and it is illustrated in Figure 2.2, where L_{ch}, L_V and L_P are the LLR values from the channel, variable node and check node respectively. This process of message passing continues until the maximum number of iterations allowed or until a codeword is successfully decoded. One such message passing algorithm used in this thesis is the Belief Propagation algorithm [7], which is based on the soft input message passing method.

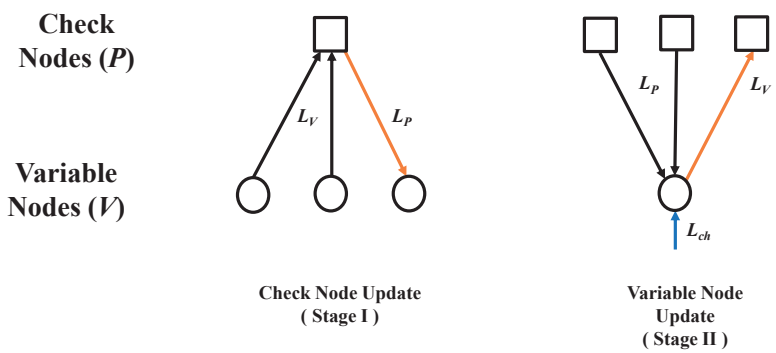

Figure 2.2: Illustration of Message Passing Algorithm.

LDPC Codes for Wi-Fi Standards

The parity check matrices of LDPC codes used in Wi-Fi standards are divided into square sub-matrices of size $Z \times Z$, and these sub-matrices are either null matrices or cyclically right-shifted (column-wise) permutation of an identity matrix [8]. In this thesis work, an LDPC code rate of 0.5 and block length of 1944 code bits is used throughout, where the sub-matrices are of size Z = 81.

2.3 Modulation Schemes

Before being transmitted, the information bits are mapped onto symbols and are then sent over the channel. The schemes which perform these mappings are commonly known as modulation schemes. The constellation diagrams are often used to represent these mappings geometrically, and the mapped symbols are referred to as constellation points. In this thesis, Quadrature Amplitude Modulation (QAM) is used, where the information bits are placed as amplitude values on the in-phase and quadrature components. Appendix A shows the constellation diagrams with Gray Mapping (i.e., no two adjacent constellation points differ by more than one bit) for different M-ary QAM, where M = 4, 16, 64 and 256.

With an aim to use the channel resources effectively, higher-order modulation is usually preferred, but the bit-error rate increases with the modulation order. To avoid these errors and achieve spectrum-efficient communication, an FEC encoder is employed with a modulator. The combination of FEC coding and non-binary modulation technique is known as Coded Modulation (CM).

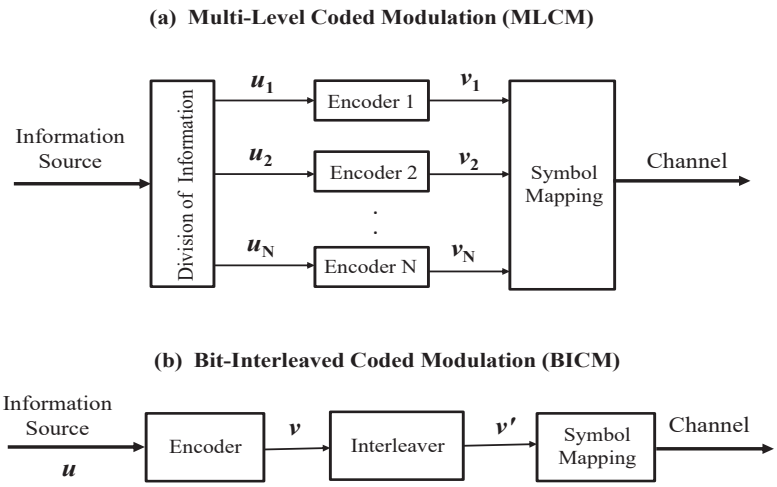

Figure 2.3: Block Diagrams of (a) Multi-level Coded Modulation (MLCM) and (b) Bit-Interleaved Coded Modulation (BICM).

The two primary coded modulation schemes which are widely in use today are Multi-Layer Coded Modulation (MLCM) and Bit-Interleaved Coded Modulation (BICM). Figure 2.3 (a) shows the block diagrams of MLCM, where $\boldsymbol{u_i}$ and $\boldsymbol{v_i}$ are input and output bits of N encoders where $i = 1, 2, \ldots, N$ and $N = \log_2(M)$ and Figure 2.3 (b) shows the block diagrams of BICM coded modulation, where $\boldsymbol{u}$ and $\boldsymbol{v}$ are input and output bits of an encoder and $\boldsymbol{v'}$ is scrambled output bits from the interleaver.

MLCM employs different code rates for each bit within a symbol. It aims to maximize the minimum Euclidean distance between the symbols in the constellation by appropriately choosing the code rate at each bit-level. However, the number of encoders and decoders increases with the higher order modulation M, thereby increasing the system complexity. Unlike MLC, BICM employs the same code rate for all bits and performs bit-interleaving before symbol mapping. The code used in BICM can be either block code or convolution code. However, when the BICM scheme is employed with LDPC code, there is no need for an interleaver as the random nature of LDPC codes guarantees the randomness between the code bits. Thus, the advantages of both MLCM and BICM with LDPC codes motivates the idea of multi-layer transmission technique to achieve reliable and spectrum-efficient communication [9] [10].

2.4 Channel Models

The propagation medium between the transmitter and the receiver over which the information is transmitted is referred to as channel. In general, it is characterized by multi-path fading, path loss due to external environments.

2.4.1 Additive White Gaussian Noise Channel

In order to visualize the channel characteristics mathematically, channel models are employed. One such model which is widely used is Additive White Gaussian Noise (AWGN) model and it is defined as follows [6],

$$y = H_{ch} \cdot x + W \tag{2.7}$$

where x is an input symbol , H_{ch} is a complex channel value and W is a complex Gaussian noise value with zero mean and variance σ^2 i.e. $W \sim \mathcal{CN}(0, \sigma^2)$. The term "white" indicates that the noise power is Independent and Identically Distributed (IID) over all the channel realizations of the type (2.7). The channel dependent Signal-to-Noise Ratio (SNR) is defined as the ratio of average symbol energy E_s to the noise variance σ^2 and it is denoted by γ. Mathematically, it is given by,

$$\gamma = \frac{E_s}{\sigma^2} = \frac{\mathbb{E}[x^2]}{\sigma^2} \tag{2.8}$$

where $\mathbb{E}$ represents the expectation operator.

Channel Capacity

The maximum rate at which the information bits are transmitted such that a very low probability of error is achievable is defined by Channel Capacity and it is denoted by C. For a given received energy γ over channel H_{ch}, the maximum transmission rate can be estimated using Shannon's channel capacity theorem and mathematically it is defined as follows [5],

$$C = \max_{p(x)} I(X;Y) = \log_2(1+\gamma) \text{ bit/channel use.} \tag{2.9}$$

Channel capacity can also be interpreted as maximizing the information of random variable X given the random variable Y such that $p(x)$ is Gaussian distributed. In this thesis, the focus is on interference that affects the performance rather than noise. It is assumed that the interference can be modelled as AWGN and hence, the equation (2.9) is still valid but Signal-to-Interference-plus-Noise Ratio (SINR), is considered in place of γ.

2.4.2 Varying Channel

The varying channel conditions can be modelled in different ways based on different situations under study, e.g., when the transmitter and/or the receiver is moving, the channel variations may be modelled as Rayleigh fading. In this thesis, the varying channel conditions are assumed to be caused by variations in the interference level at the receiver and hence, the channel can be modelled as block fading channel, i.e., the channel variations (i.e., SINR) remain constant during transmission of a packet, however, it may vary from one packet to another. In order to mimic the varying nature of the channel for different transmissions, the actual SNR is uniformly varied by 0 dB or 10 dB during the simulation.

2.5 ARQ and HARQ Schemes

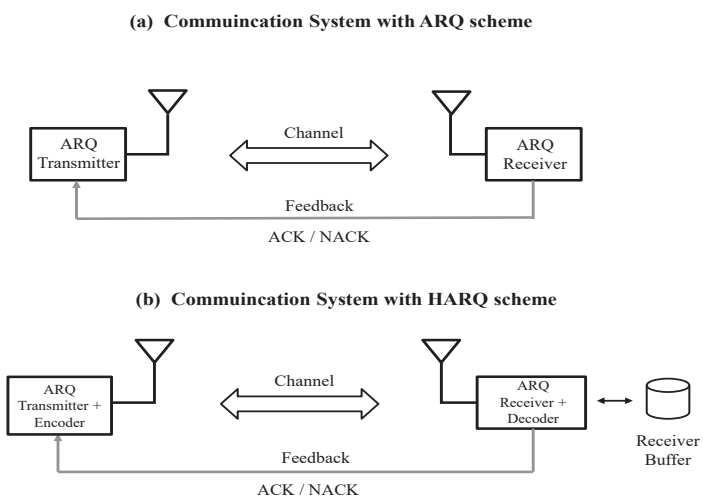

Figure 2.4: Block diagrams of basic communication system with (a) ARQ scheme and (b) HARQ scheme.

The channel errors caused during the data transmission can also be controlled using a retransmission mechanism called Automatic Repeat reQuest (ARQ). If the received data contain error(s), then the ARQ scheme at the receiver side requests transmitter to retransmit the data again using a negative acknowledgment (NACK). If the received data has no error, then an acknowledgment (ACK) is sent to the transmitter, indicating that it has successfully received the data. However, it introduces a larger delay due to retransmissions in case of bad channels. In order to exploit the benefits of both FEC coding and ARQ schemes, both functionalities are combined, and it is referred to as a hybrid-ARQ (HARQ) scheme. The HARQ schemes employ receiver buffers to combine the LLRs of different (re)transmissions to control the bit errors suffered over the channel. Figure 2.4 (a) and Figure 2.4 (b) show the block diagrams of communication systems employing ARQ and HARQ scheme respectively.

There are two main types of HARQ schemes: HARQ-Chase Combing scheme (HARQ-CC) and HARQ-Incremental Redundancy scheme (HARQ-IR). In the event that the data is correctly received, then both the types of HARQ schemes request for new data. However, in the event that the data has error(s), then in the HARQ-CC scheme, the received information is stored, and it is then combined with retransmitted information, thereby increasing the received energy of information. When sufficient energy is accumulated, the original data is successfully recovered. In the case of the HARQ-IR scheme, specific redundancy bits are retransmitted instead of retransmitting the same data in case of packet failure. This additional redundancy, when combined with the original data, lowers the effective code rate, thus attempting to recover the original data. Throughout this thesis work, the HARQ-CC scheme has been employed [11].

Chapter 3

Received Bit Information Rate

The objective of a transmission technique is to achieve a very low or zero probability of error. In order to fulfill this, it is important that for a given transmission technique, coding and modulation parameters are carefully selected. Hence, for given channel conditions at the receiver, there is a need for a model to understand how the transmission information rate and modulation technique influence the performance of the receiver. One such model is based on Received Bit Information Rate (RBIR) metric, which is discussed in detail in this chapter.

3.1 Introduction

The information about the transmitted bit within a given symbol obtained by observing the corresponding received bit is termed as RBIR, and it is denoted by Φ. For any binary FEC, the RBIR sets an upper limit on the coding rate r such that codeword is correctly decoded i.e., $\Phi >= r$. For a given channel-dependent SNR, γ, and modulation order of M, mathematically RBIR Φ for each bit within a symbol [12] is given by

$$\Phi_k = 1 - \frac{1}{M}\sum_{i=1}^{M} \mathbb{E}_W \left[\log_2 \left(1 + \frac{\sum_{j=1;b_{kj}\neq b_{ki}}^{M} e^{(|W|^2 - |\sqrt{\gamma}(x_j - x_i) + W|^2)}}{\sum_{j=1;b_{kj}=b_{ki}}^{M} e^{(|W|^2 - |\sqrt{\gamma}(x_j - x_i) + W|^2)}} \right) \right]. \quad (3.1)$$

where b_{ki} and b_{kj} are transmitted and received bits corresponding to their transmitted and received symbols x_i and x_j respectively, where W is the zero mean complex Gaussian noise with unit variance (i.e., $\sigma^2 = 1$), $\mathbb{E}_W$ represents the expectation over the W and $k = 1, 2, \ldots, \log_2(M)$.

The above equation is an effective evaluation of equation (2.5), where the two terms on right-hand side of equation (3.1) correspond to $H(X)$ and $H(X|Y)$, respectively.

The sum of RBIR of each bit Φ_k within a symbol is represented as follows,

$$\Phi_{sum} = \sum_{k} \Phi_k. \quad (3.2)$$

3.1.1 RBIR Derivation

The RBIR definition can also be extended to a symbol by normalizing the Symbol-level mutual Information (SI) by number of information bits per symbol [12]. The normalized RBIR based on SI is given by

$$\Phi_{norm} = \frac{SI}{\log_2 M}. \tag{3.3}$$

As per the information theory (Section 2.1), the mutual information of transmitted symbol x obtained by observing the received symbol y is given by

$$SI = I(X;Y) = \sum_{x\epsilon X}\sum_{y\epsilon Y} p(y|x)p(x)\log_2 \frac{p(y|x)}{p(y)}. \tag{3.4}$$

Assuming the transmitted symbols are equi-probable i.e. $p(x) = \frac{1}{M}$, the term $\frac{p(y|x)}{p(y)}$can be written in relation to symbol-level log likelihood ratio (LLR) as

$$\frac{p(y|x)}{p(y)} = \frac{M}{1+e^{-LLR}}. \tag{3.5}$$

Substituting (3.5) into (3.4), we get

$$SI = \log_2(M) - \frac{1}{M}\sum_{i=1}^{M} \mathbb{E}_y\left[\log_2(1+e^{-LLR_i})\right]. \tag{3.6}$$

where LLR_i represents symbol-level LLR and $i = 1, 2, \ldots, M$,

$$LLR_i = \log_e\left[\frac{p(x=x_i|y)}{\sum_{k=1,k\neq i}^{M} p(x=x_k|y)}\right] = \log_e\left[\frac{e^{\frac{-d_i^2}{\sigma^2}}}{\sum_{k=1,k\neq i}^{M} e^{\frac{-d_k^2}{\sigma^2}}}\right]. \tag{3.7}$$

and $d_i^2 = ||y - H_{ch}x_i||^2$ is the Euclidean distance between the received symbol y and the transmitted symbol x_i and $i = 1, 2, ...M$. The received symbol y follows the channel model described in Section 2.4.1, where W is the zero mean complex Gaussian noise with $\sigma^2 = 1$.

The symbol level mutual information can be generalized using (3.6) and (3.7) as follows,

$$SI = \log_2(M) - \frac{1}{M}\sum_{i=1}^{M} \mathbb{E}_W\left[\log_2\left(1 + \sum_{j=1,j\neq i}^{M} e^{(|W|^2 - |\sqrt{\gamma}(x_j - x_i) + W|^2)}\right)\right] \tag{3.8}$$

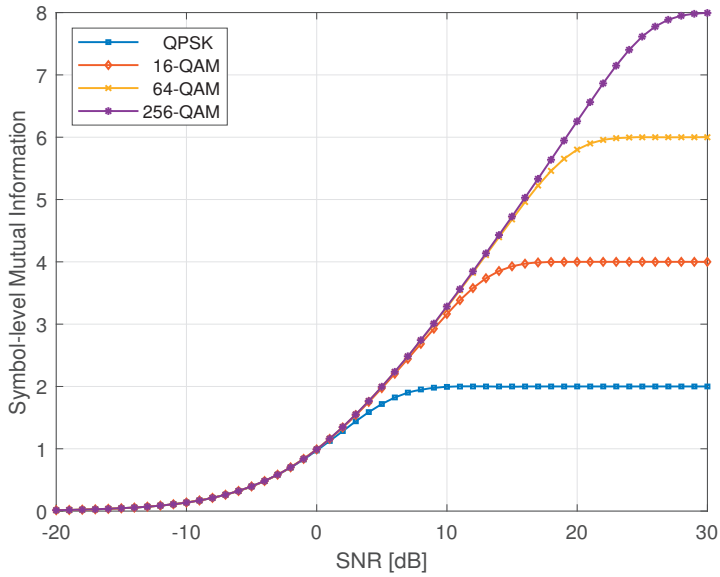

Figure 3.1: Symbol Level Mutual Information for M = 4, 16, 64, 256.

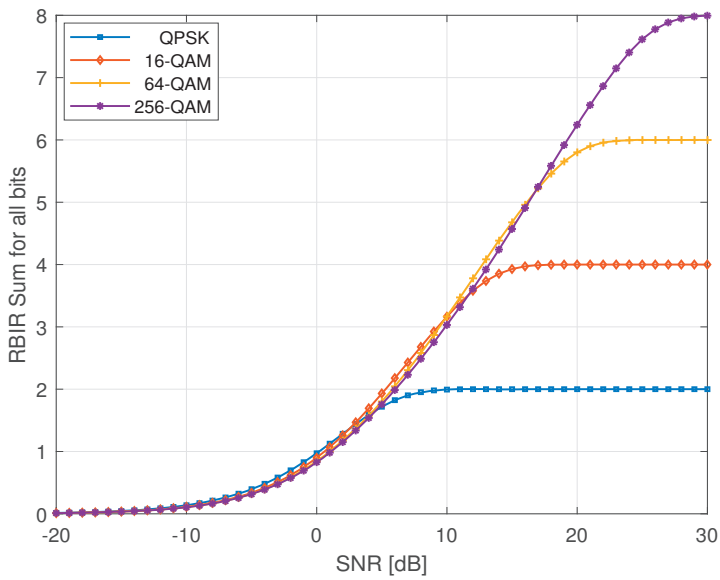

Figure 3.2: Sum of Bit Level Mutual Information of all bits for M = 4, 16, 64, 256.

The numerical evaluations of sum of bit-level mutual information and SI for different M-ary QAM schemes using (3.2) and (3.8), are shown in Figure 3.1 and Figure 3.2 respectively. It is seen that the sum of RBIR of all bits for different modulations suffers from a minor loss in information by choosing higher modulation when compared to SI. Figure 3.3 illustrates the gap between SI and the sum of RBIR of all bits for 256-QAM. This gap, due to minor loss of information, can be avoided by using a successive cancellation method, which is described in more detail in Chapter 6.

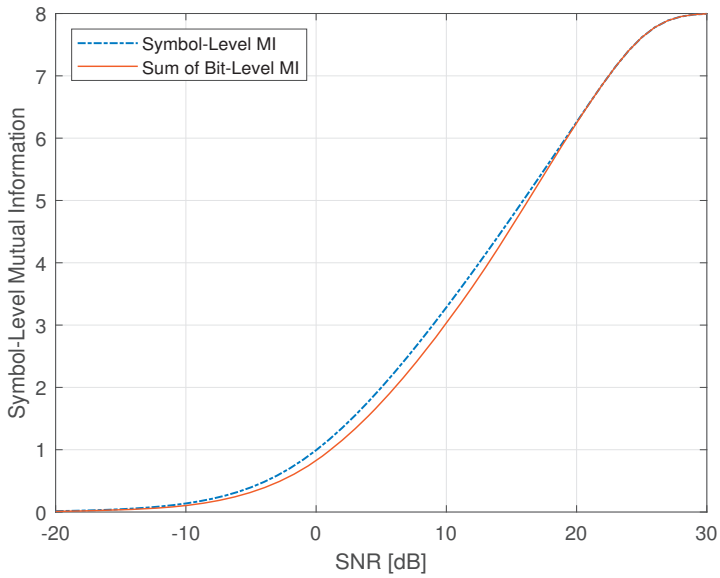

Figure 3.3: Comparison of Symbol Level MI and sum of RBIR of all bits for M = 256.

3.2 Bit Reliabilities using RBIR

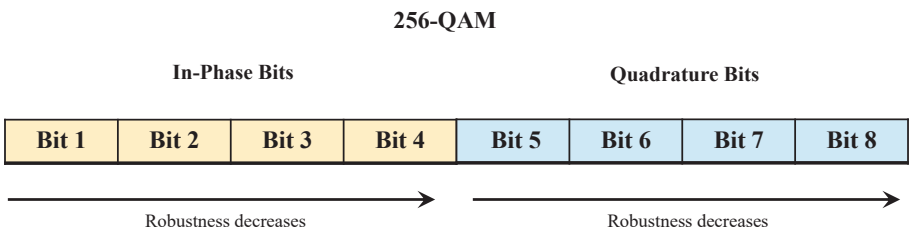

Figure 3.4: In-phase and quadrature bits of 256-QAM for Gray mapping defined in Appendix A.1.4.

For any Gray mapping used in M-ary QAM, bits within a symbol can be grouped into in-phase and quadrature bits. Since the in-phase and quadrature bits of modulated symbols are orthogonal, there are two sets of received bits which carry the same amount of information defined by RBIR. The in-phase and quadrature bits for 256-QAM using Gray mapping defined in Appendix A.1.4 are shown in Figure 3.4.

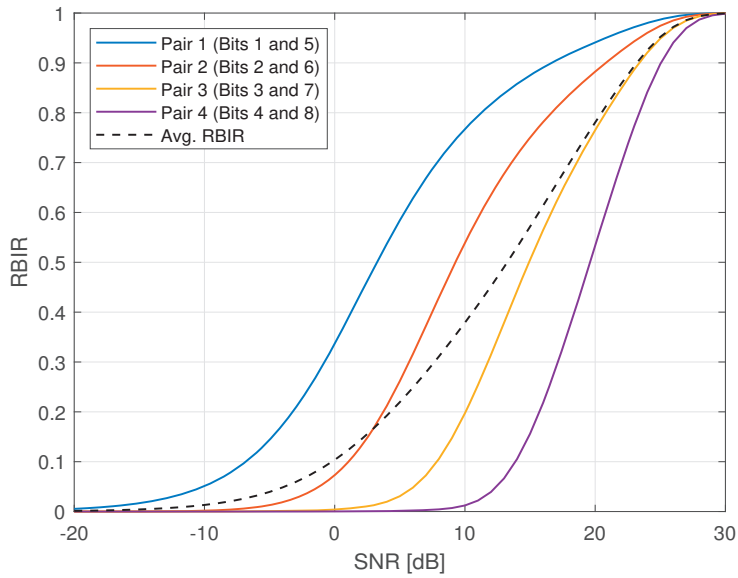

Figure 3.5: Comparison of bit-wise RBIR and average RBIR within a symbol for M = 256.

The amount of information carried by bits 1 and 5, bits 2 and 6, bits 3 and 7, and bits 4 and 8 are same and hence the RBIR curves in Figure 3.5 are overlapping for the two bits in respective pairs. It is important to note that based on the particular Gray mapping used, the bit pairs are defined. Bits 1 and 5 are considered to be the most robust bits as they are more reliable when compared to the least robust bits 4 and 8 by at least 17 dB as per the Figure 3.5. The remaining bits 2 and 6 and bits 3 and 7 are with intermediate robustness.For traditional transmission technique, the average RBIR is considered, and it is shown in Figure 3.5 using a dashed line.

In this thesis work, all the results are simulated for 256-QAM as it provides more degrees of freedom to analyse how much information each bit carries and how this bit information can be further exploited. As per the Figure 3.5, for a code rate of 0.5, the theoretical SNR required to successfully decode bits belonging to pair 1 (i.e., bit 1 and bit 5), pair 2 (i.e., bit 2 and bit 6), pair 3 (i.e., bit 3 and bit 7) and pair 4 (i.e., bit 4 and bit 8) are found to be around 4 dB, 10 dB, 15 dB and 20 dB respectively. The MLT technique is very much about how these different bit reliabilities can be explored to achieve better performance than traditional transmission techniques.

3.3 Relation between RBIR and HARQ schemes

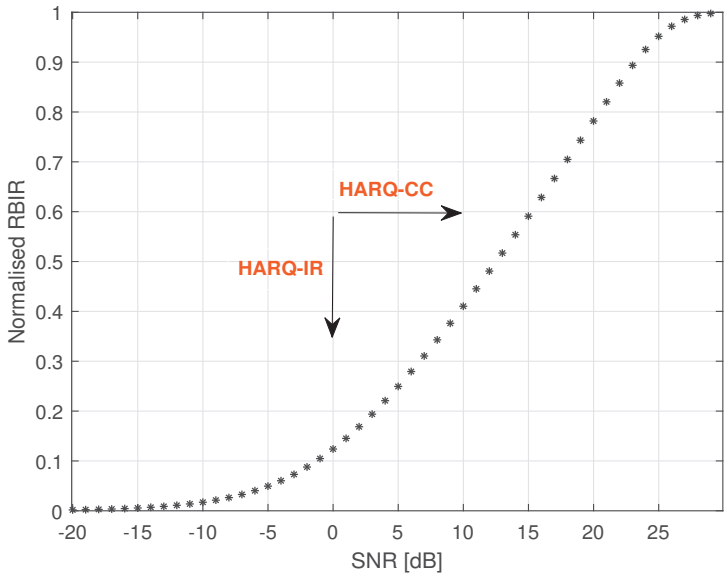

Figure 3.6: Illustration of relation between RBIR and HARQ schemes.

When the HARQ-CC scheme is employed, each re-transmission results in the accumulation of received energy, which in turn implies the accumulation of RBIR. Hence, choosing a high code rate results in need for more re-transmissions until sufficient energy is accumulated, whereas choosing a low code rate results in inefficient use of channel capacity. Thus a moderately low code rate is preferred in the case of HARQ-CC. In contrast, each re-transmission in the case of the HARQ-IR scheme results in reducing the code rate, and therefore choosing a high code rate is not much of a penalty. However, selecting a low code rate in the case of the HARQ-IR scheme follows the same conclusion as in the case of the HARQ-CC scheme. Thus, it effectively implies that each re-transmission results in traversing the RBIR curve horizontally for HARQ-CC scheme and vertically for HARQ-IR scheme and this has been illustrated in Figure 3.6.

Chapter 4

Multi-Layer Transmission

A major challenge in the design of wireless communication systems is how to estimate the channel conditions at the transmitter side when the channel is changing fast. Even by employing a link adaptation technique at the transmitter, it is nearly impossible to predict the CSI when the feedback information from the receiver gets outdated very quickly. To address this issue, a Multi-Layer Transmission (MLT) technique using HARQ schemes have been introduced such that the channel is used in an opportunistic way, thereby removing the need for link adaptation.

4.1 Structure of MLT

MLT technique is conceptually characterized by a set of layers over which codewords of equal block length are sent. The number of m codewords sent per each transmission over their corresponding m layers is dependent on the M-ary constellation used in the modulation process where $m = \log_2 \mathrm{M}$. Hence, MLT technique can also be termed as Multi-Layer Modulation technique. Each layer in MLT corresponds to each bit of an M-ary modulated symbol, over which codewords are sent. Therefore, the robust bits, as described in Section 3.2 w.r.t Figure 3.5, are often referred to as robust layers in MLT, and thus the layers 1 and 5 and layers 4 and 8 are considered as the most robust and the least robust layers, respectively.

Traditionally, codewords are fed sequentially, i.e., one after the other to the modulator, whereas, in MLT transmission, codewords are fed in parallel (i.e., each bit from each codeword is fed to the modulator). Figure 4.1 illustrates the traditional and multi-layer transmission ways of modulating codewords (codeword 1 and codeword 2) using a 4-QAM modulator. The resulting modulated symbols in case of traditional approach are as follows, s_1, s_4, s_2, s_3 whereas in case of multi-layer approach, the resulting modulated symbols are s_3, s_1, s_2, s_4. These symbols are then sent over the channel. It is assumed that the channel remains constant over each transmission; however, it may vary between the transmissions.

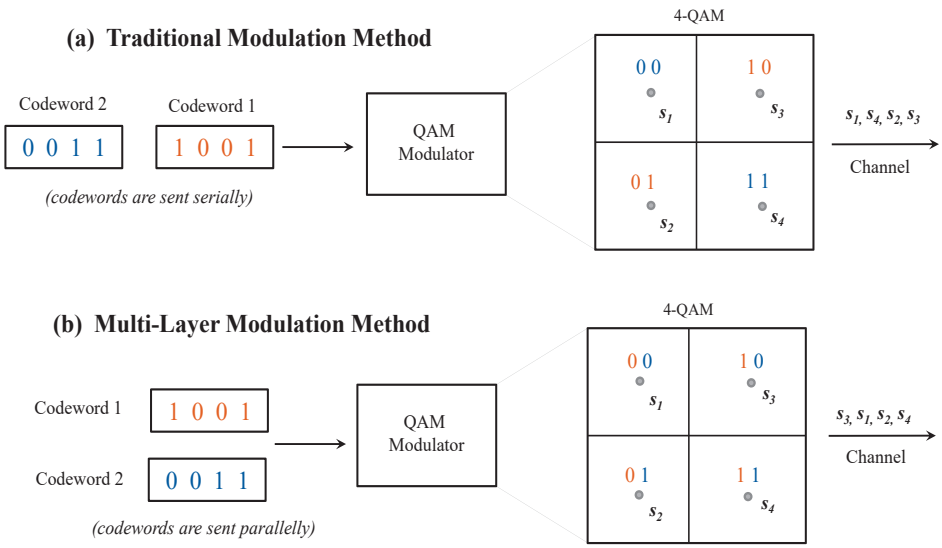

Figure 4.1: Modulation methods for (a) Traditional approach and (b) MLT approach.

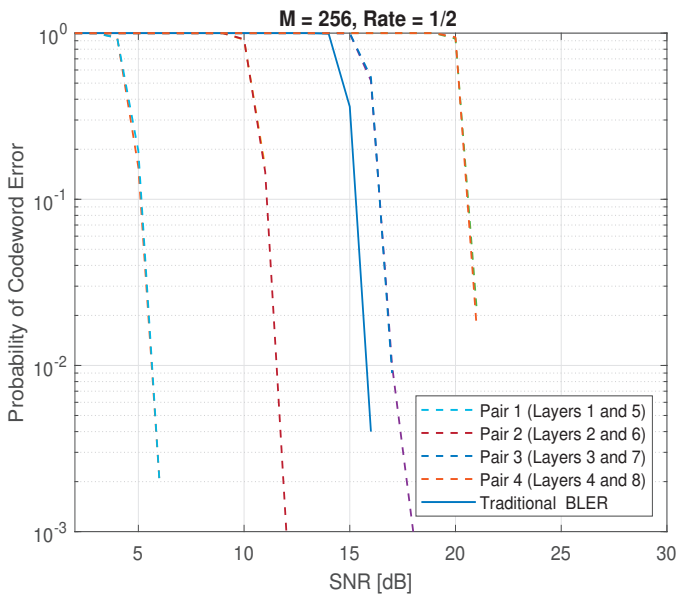

Figure 4.2: Comparison of codeword error probability for different layers in MLT and the traditional approach.

To appreciate the difference between MLT and the traditional approach, the probability of codeword error (often referred as BLock Error Probability (BLER)) for different layers in the MLT technique are compared with the traditional approach. Figure 4.2 shows the block error probability over the AWGN channel for 256-QAM with LDPC code of block length 1944 and rate $r = 0.5$ as defined in Section 2.2.1. The different layers in MLT require around 6 dB, 12 dB, 17 dB, and 21 dB for successful decoding of the codewords on their respective layers, whereas the traditional approach requires 16 dB. It is observed that the practical threshold of each pair of layers in Figure 4.2 has been shifted by at least 1-2 dB when compared to theoretical thresholds discussed in Section 3.2 with respect to Figure 3.5.

SNR Threshold	**Pair 1**	**Pair 2**	**Pair 3**	**Pair 4**
Theoretical	4 dB	10 dB	15 dB	20 dB
Practical	6 dB	12 dB	17 dB	21 dB

Table 4.1: Summary of theoretical and practical SNR thresholds for each pair of layers in MLT technique.

The theoretical and practical thresholds in SNR for each pair of layers in MLT approach are summarized in Table 4.1. It is also seen that, there is an average increase in the RBIR threshold by 9% of the code rate for all the pairs. Thus, for a LDPC code of block length 1944 of rate 0.5, RBIR must be at least 0.545 for a codeword to succeed. Note that the total RBIR is not impacted by MLT technique; however, MLT guarantees that the codewords that are sent on the robust layers are more likely to be successfully decoded.

Each layer in MLT supports the HARQ scheme independently, and therefore none of the codewords on their respective layers impact each other. When the received codeword is successfully decoded, a new codeword is sent on its corresponding layer. In the event that the received codeword is corrupted, the receiver employs the HARQ-CC scheme and requests for retransmission of the same codeword on the same layer until the codeword is successfully decoded. This effectively implies accumulation of RBIR over each retransmission. Thus, at a given SNR, for every two transmissions of a codeword on the same layer, the SNR increases by 3 dB because of the chase combining mechanism. For instance, if a codeword $\boldsymbol{v}$ is transmitted over layer 1 using MLT technique at 3 dB, then after two transmissions of the same codeword $\boldsymbol{v}$ over the same layer, the accumulated SNR is approximately equal to 6 dB (i.e. 3 dB + $10 \cdot \log_{10}(2)$).

4.1.1 MLT Process

The step-by-step process of using MLT in combination with the HARQ-CC scheme has been summarized in a flow chart shown in Figure 4.3.

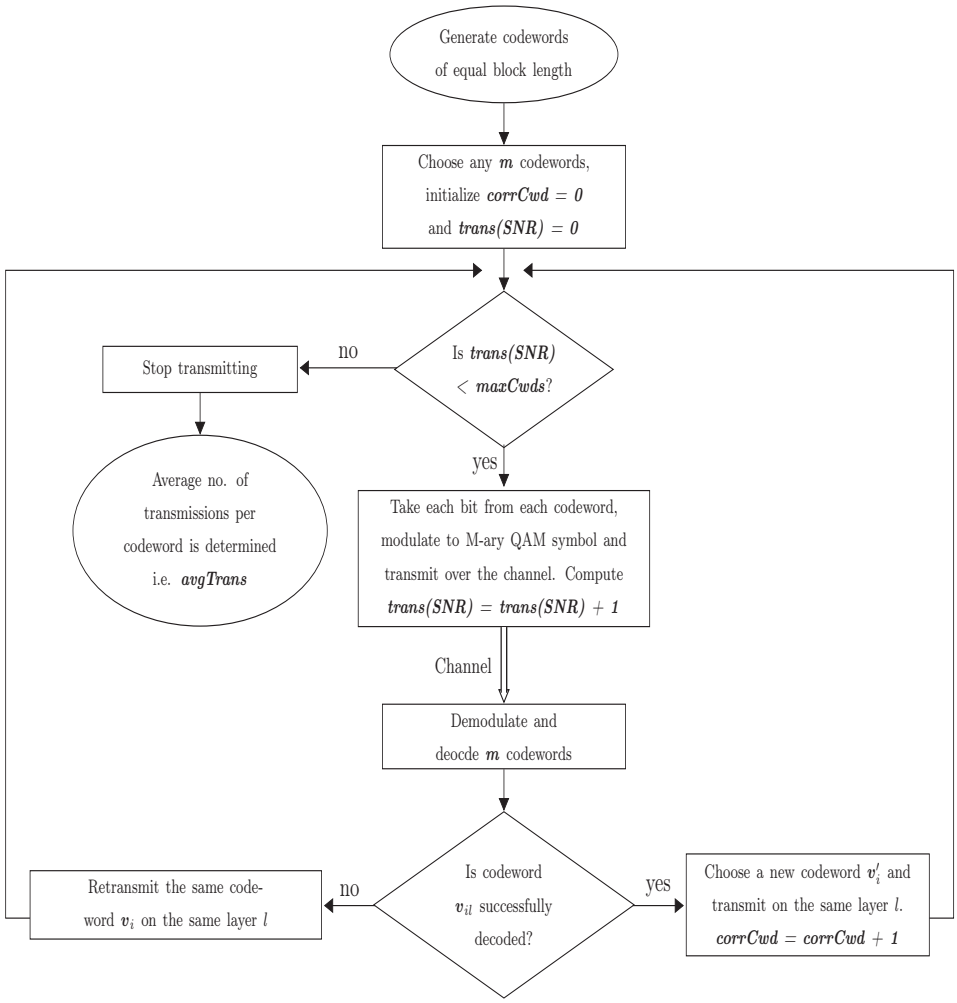

Figure 4.3: Flow Chart for Multi-Layer Transmission Process.

The counters $\boldsymbol{corrCwd}$ and $\boldsymbol{trans(SNR)}$ are defined in order to keep track of total number of successfully decoded codewords and the total number of transmissions required to successfully decode a codeword $\boldsymbol{v}_i$ on layer l at a given SNR, respectively and are initialized to zero before transmission, where $i, l = 1, 2, \ldots, \log_2 M$. As per MLT, m codewords of equal block length are generated and are sent in parallel over the channel as illustrated in Figure 4.1 (b), where $m = \log_2(M)$. Note that the notation $\boldsymbol{v}_{il}$ means that a codeword $\boldsymbol{v}_i$ is transmitted on layer l.

At the receiver side, the received information at SNR is demodulated and then decoded into m codewords. If the received codeword $\boldsymbol{v}_i$ on layer l is successfully decoded, then a new codeword $\boldsymbol{v}_i'$ is transmitted on layer l and the counter $\boldsymbol{corrCwd}$ is incremented by 1. In the event that the received codeword $\boldsymbol{v}_i$ is corrupted on layer l, then the same codeword $\boldsymbol{v}_i$ is retransmitted on layer l and the counter $\boldsymbol{trans(SNR)}$ is incremented by 1. This process continues until the

counter ***corrCwd*** reaches the required maximum number of codewords defined as ***maxCwds***. When the counter ***corrCwd*** reaches ***maxCwds***, the transmission is stopped and the average number of transmissions per codeword require to successfully decode ***maxCwds*** number of codewords is determined.

4.2 Performance of MLT

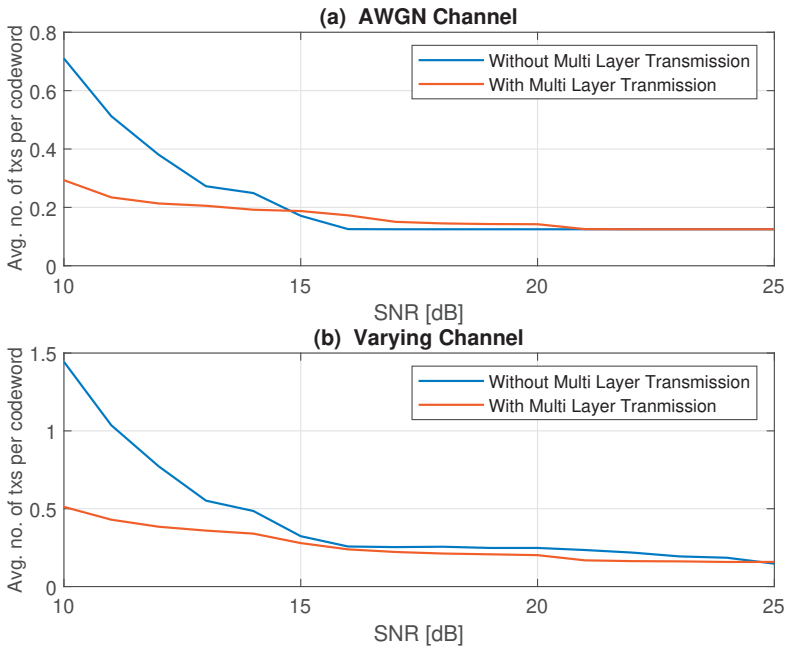

Figure 4.4: Performance of MLT over (a) AWGN channel and (b) Varying channel.

The performance of MLT in combination with HARQ-CC compared to the traditional approach is measured based on the total number of transmissions required to correctly decode a given number of codewords. The simulations are performed based on the algorithm defined in Figure 4.3 to successfully decode 10000 codewords. For an AWGN channel, it is observed from Figure 4.4 (a) that the MLT outperforms traditional transmission technique for AWGN channel over moderately lower SNR range (i.e., below 14.5 dB), however, over a range of 15 dB - 22 dB, the number of transmissions required in case of MLT goes beyond the traditional approach as the less robust layers in MLT fail to recover from bad channel conditions. Thus, it is advantageous to employ MLT over the AWGN channel for lower SNR range such that the need for link adaptation is removed. However, for SNR range of 15 dB - 20 dB, it is reasonable to adopt a link adaptation technique and employ traditional transmission technique.

For varying channel, MLT transmission outperforms traditional transmission techniques over the entire SNR range and it is shown in Figure 4.4 (b). Thus, MLT transmission completely removes the need for link adaptation over the varying channel and thus reducing the complexity at both transmitter and receiver sides.

Example 4.1

For instance, consider MLT transmission of two codewords, say, $\boldsymbol{v}_1$ and $\boldsymbol{v}_2$ are being sent on layer 1 and layer 2 respectively, over AWGN channel at SNR of 10 dB. Assume that a code rate of 0.5 and 256-QAM modulation is used. From Figure 3.5, the approximate RBIR values of Pair 1, Pair 2 , Pair 3 and Pair 4 at 10 dB for rate $r = 0.5$ are found to be 0.76, 0.539, 0.198 and 0.012 respectively. The codeword $\boldsymbol{v}_1$ on layer 1 is successfully decoded as the RBIR at 10 dB for layer 1 exceeds the practical threshold of 0.545. However, the codeword $\boldsymbol{v}_2$ on layer 2 fails and thus it is requested for re-transmission on the same layer at 10 dB. Since HARQ-CC scheme is employed throughout, after two transmissions in total, the accumulated SNR is found to be 13 dB which corresponds to RBIR of 0.68 on layer 2.

$$\begin{aligned} \text{Accumulated SNR on layer 2} &= 10 \text{ dB} + 10 \cdot \log_{10}(2) \\ &= 13 \text{ dB} \end{aligned}$$

Since it exceeds the required practical threshold, the codeword on the layer 2 is successfully decoded. However, it is important to note that the channel capacity must be used optimally and thus the re-transmission of codewords should aim at accumulating RBIR which is just sufficient enough to achieve successful decoding. This motivates of idea of mixing layers which is discussed in detail in next chapter.

Thus, to summarize the findings from the above simulation results, MLT technique exploits the varying channel opportunistically without the need for link adaptation and provides better performance than the traditional transmission technique in terms of number of transmissions required per codeword. Furthermore, the concept of different bit reliabilities, which has been explored in MLT transmission motivates to investigate the different variants of MLT transmission techniques.

Chapter 5

Further Improvements on Multi-Layer Transmission

In this chapter, the concepts of RBIR are further exploited in MLT transmission with an aim to efficiently use the channel resources. The idea of employing successive demodulation in MLT is briefly discussed. Furthermore, the performance of MLT along with ARQ scheme is investigated.

5.1 Mixing Layers

As we discussed in previous chapter, the MLT technique along with HARQ-CC scheme results in accumulation of RBIR over each retransmission in case erroneous reception of a codeword. Each retransmission must aid the codeword on a particular layer to succeed and accumulate just sufficient RBIR (i.e. at least equal to code rate) such that the channel resources are efficiently used. Thus, when a codeword on particular layer, after certain number of transmission(s), has accumulated RBIR which is very close to the code rate used, then it is wise to choose less robust layer for re-transmission, thereby giving a little nudge for the codeword to accumulate sufficient RBIR. This concept of using different layer for retransmission is termed as "Mixing Layers". The pre-determined values of RBIR for each layer with respect to Figure 3.5 are used in order to determine whether the particular codeword on a given layer has accumulated enough RBIR for a given effective channel SNR.

5.1.1 Process of Mixing Layers

The entire process of mixing layers is described in a flow chart shown in Figure 5.1. The process follows the standard MLT approach described in Figure 4.3 with minor modifications. The counter $\boldsymbol{trans(v_{il}, SNR)}$ is defined for each layer to keep track of total number of transmissions required to successfully decode a codeword $\boldsymbol{v}_{il}$ on that particular layer at a given SNR and it is of size $1 \times \boldsymbol{m}$, where $\boldsymbol{m} = \log_2(M)$. Before transmission of $\boldsymbol{m}$ codewords, the flag $\boldsymbol{mix}$ is initialized to 0. During the first transmission, no mixing of layers is performed and the counter $\boldsymbol{trans(v_{kl}, SNR)}$ is incremented by 1 for each layer.

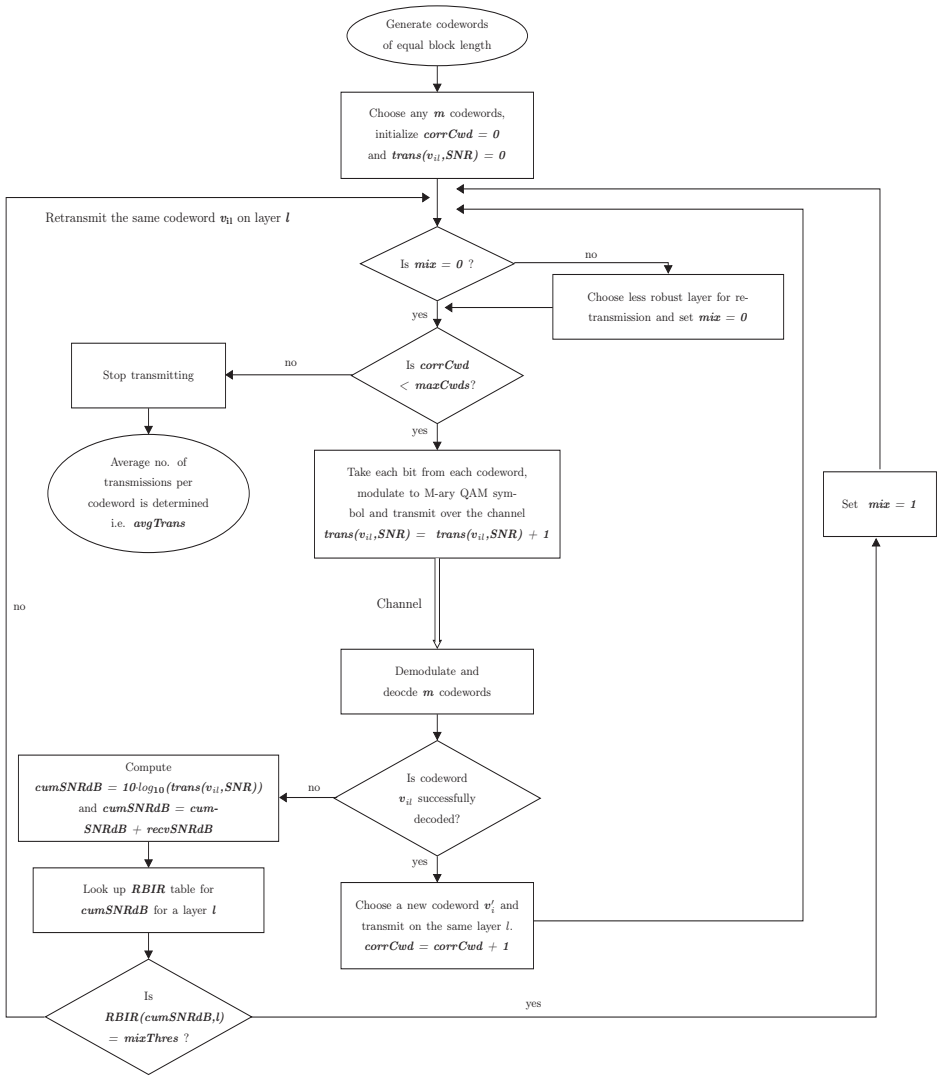

Figure 5.1: Flow Chart for Mixing Layers in MLT.

The received codewords at SNR $\boldsymbol{recvSNRdB}$ are demodulated and decoded at the receiver. On successful decoding of each received codeword $\boldsymbol{v}_{il}$, the counter $\boldsymbol{corrCwd}$ is incremented and a new codeword $\boldsymbol{v}'_{il}$ is then sent on its respective layer. In case that the received codeword on a layer l is not successfully decoded, the cumulative SNR $\boldsymbol{cumSNRdB}$ is determined using the transmission counter value $\boldsymbol{trans(v_{il}, SNR)}$ for a codeword $\boldsymbol{v}_{il}$ on that layer l as shown in Figure 5.1. Using the predetermined RBIR values, the value $\boldsymbol{RBIR(cumSNRdB, l)}$ at calculated $\boldsymbol{cumSNRdB}$ is determined for layer l. In order to effectively use the channel capacity, the RBIR value, close to code rate, is used to define a threshold for choosing the different layer for retransmission and it is denoted by $\boldsymbol{mixThres}$. If the $\boldsymbol{RBIR(cumSNRdB, l)}$ is equal to $\boldsymbol{mixThres}$, then the flag $\boldsymbol{mix}$ is set to

1 indicating that the codeword needs to be transmitted on the less robust layers. If the $\boldsymbol{RBIR(cumSNRdB, l)}$ is not equal to $\boldsymbol{mixThres}$, then the codeword is requested for retransmission on the same layer to accumulate sufficient RBIR.

Before every transmission, the value of flag $\boldsymbol{mix}$ is checked. If the flag $\boldsymbol{mix}$ is set to 1, then the less robust layer $l+1$ is used for retransmitting the codeword $\boldsymbol{v}_{il}$ and the layer l is used retransmitting the codeword $\boldsymbol{v}_{i(l+1)}$. After mixing layers, the counters $\boldsymbol{trans(v_{kl}, SNR)}$ and $\boldsymbol{trans(v_{k(l+1)}, SNR)}$ are reinitialized to 0 and the flag $\boldsymbol{mix}$ set to 0.

This process continues until the counter $\boldsymbol{corrCwd}$ reaches the required maximum number of codewords defined by $\boldsymbol{maxCwds}$. When the counter $\boldsymbol{corrCwd}$ reaches $\boldsymbol{maxCwds}$, the transmission of codewords is stopped and the average number of transmissions per codeword require to successfully decode $\boldsymbol{maxCwds}$ number of codewords is determined.

5.1.2 Performance of Mixing Layers

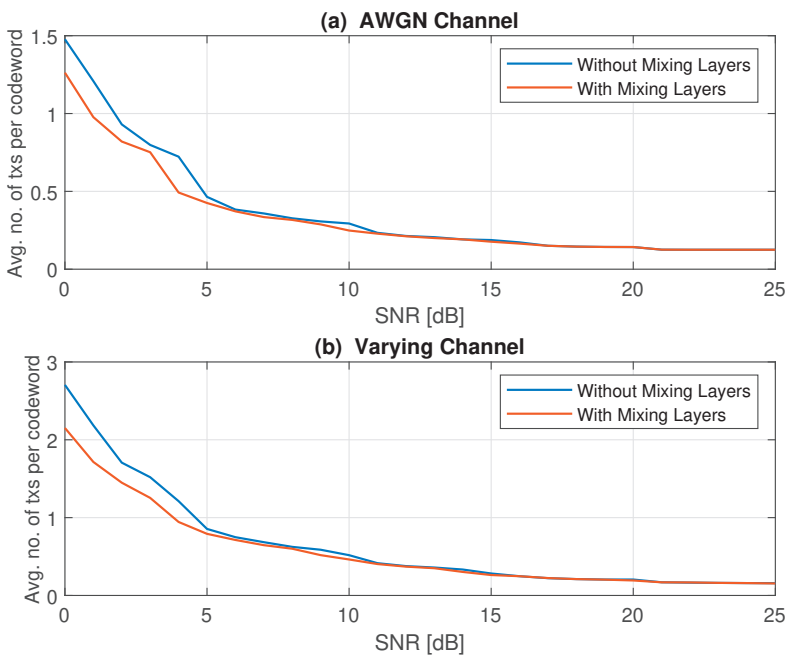

Figure 5.2: Comparison of performance of Mixing layers over (a) AWGN Channel and (b) Varying Channel.

The performance of mixing of layers is measured in terms of average number of transmissions required to successfully decode 10000 codewords and it is compared with the traditional MLT approach. Figure 5.2 (a) shows the performance for both scenarios. It is seen that mixing of layers has a noticeable gain over traditional MLT transmission especially in the lower SNR region (0-5 dB). This is because

the first two pair of robust layers are effectively utilised as much as the channel allows. However, the gain decreases towards the higher SNR region as each layer has sufficient energy to succeed in very few transmission(s) and thereby reducing the possible gain of mixing layers. Beyond 18 dB, only the least robust layers are yet to be successful and therefore, there are no more less robust layers to perform mixing. In the case of varying channel, the performance is very similar to AWGN channel and the simulation results are shown in Figure 5.2 (b). The different pairs of layers used while mixing layers for different ranges of SNR are summarised in table below.

Mix Layers	**SNR Range**
Pair 1 and Pair 2	0-5 dB
Pair 2 and Pair 3	6-11 dB
Pair 3 and Pair 4	12-18 dB

Table 5.1: Summary of different pairs of layers used during mixing layers for different SNR range.

Example 5.1

Now consider the same scenario as described in Example 4.1 On the first transmission of codeword $\boldsymbol{v}_2$ at 10 dB on the layer 2, the RBIR is about 0.539 which is less than the required practical threshold of 0.545 and thus the codeword $\boldsymbol{v}_2$ fails. As discussed, the accumulated RBIR by retransmitting $\boldsymbol{v}_2$ on layer 2 is 0.68 which corresponds to 13 dB and it is successfully decoded. Now, in order to utilize the channel capacity efficiently, instead of retransmitting $\boldsymbol{v}_2$ on the same layer, consider selecting layer 3 or layer 4 for retransmission.

Consider layer 3 for retransmitting the codeword $\boldsymbol{v}_2$. Using Figure 3.5, it is found that the the RBIR value for the first transmission on layer 2 at 10 dB is equivalent to that of the first transmission on layer 3 at 16 dB. Thus, when the codeword $\boldsymbol{v}_2$ is retransmitted on the layer 3, the accumulated SNR is calculated by adding the SNR for each transmission in linear scale and converting it back to decibels. It is found the accumulated SNR is 17 dB and the corresponding RBIR value is 0.62.

$$\begin{aligned}\text{Accumulated SNR on layer 3} &= 10\cdot\log_{10}\left(10^{\frac{10\text{ dB}}{10}} + 10^{\frac{16\text{ dB}}{10}}\right)\\ &= 17\text{ dB}\end{aligned}$$

Now, consider layer 4 for retransmitting the codeword $\boldsymbol{v}_2$. It is found that the the RBIR value for the first transmission on layer 2 at 10 dB is equivalent to that of the first transmission on layer 4 at 20 dB. Thus, when the codeword $\boldsymbol{v}_2$ is retransmitted on the layer 4, the accumulated SNR is found to be 20.4 dB and the corresponding RBIR value as per the Figure 3.5 is 0.56.

$$\begin{aligned}\text{Accumulated SNR on layer 4} &= 10\cdot\log_{10}\left(10^{\frac{10\text{ dB}}{10}} + 10^{\frac{20\text{ dB}}{10}}\right)\\ &= 20.4\text{ dB}\end{aligned}$$

Layers	Actual SNR	Accumulated SNR	Accumulated RBIR
Layer 2	10 dB	13 dB	0.67
Layer 3	16 dB	17 dB	0.62
Layer 4	20 dB	20.4 dB	0.56

Table 5.2: Summary of accumulated SNR and accumulated RBIR for layers 2, 3 and 4 used in illustrating the Example 5.1.

The effective SNR and its corresponding RBIR value for different layers used for retransmitting the codeword $\boldsymbol{v}_2$ is summarized in Table 5.2. Thus, it is reasonable to use layer 4 for retransmission of codeword $\boldsymbol{v}_2$ as the accumulated RBIR (i.e., 0.56) exceeds the practical threshold of 0.545 by very small margin.

5.2 Successive Demodulation

As discussed in Chapter 3, the sum of RBIR for all bits in Figure 3.3 suffers from minor loss when compared to SI. In order to compensate this loss, the concept of chain rule of mutual information (Section 2.1.2) is used, as the bits within the symbol are independent from each another. Thus the chain rule helps to extract the information about the less robust bits given the information of the most robust bits. The process of employing the chain rule of mutual information (successive cancellation criteria) during the demodulation of less robust bits on successful reception of the most robust bits is termed as Successive Demodulation.

When the most robust bit is successfully received, the information of this bit is used for demodulation of less robust bits. This process continues until the last bit within the symbol is demodulated. Intuitively, the constellation points are reduced at each time successive demodulation is applied at each layer. However, when the most robust bits are not decoded successfully, then the demodulation of less robust bits are carried out independently i.e. without using any information about the most robust bits and it is referred to as Parallel Demodulation.

The RBIR for each bit is calculated using successive demodulation process based on equation (2.6) and (3.1) and it is denoted as $\Phi_k^{(succ)}$, where k varies from 1 to $\log_2(M)$.

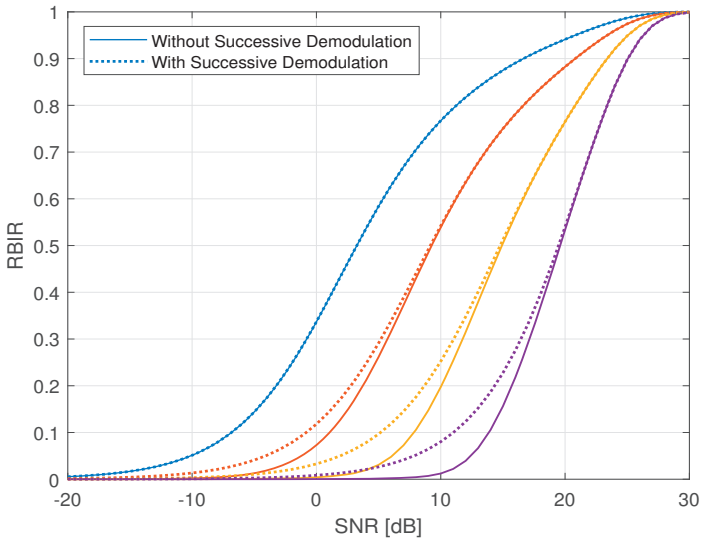

Figure 5.3: Comparison of bit-reliablities with and without employing successive demodulation.

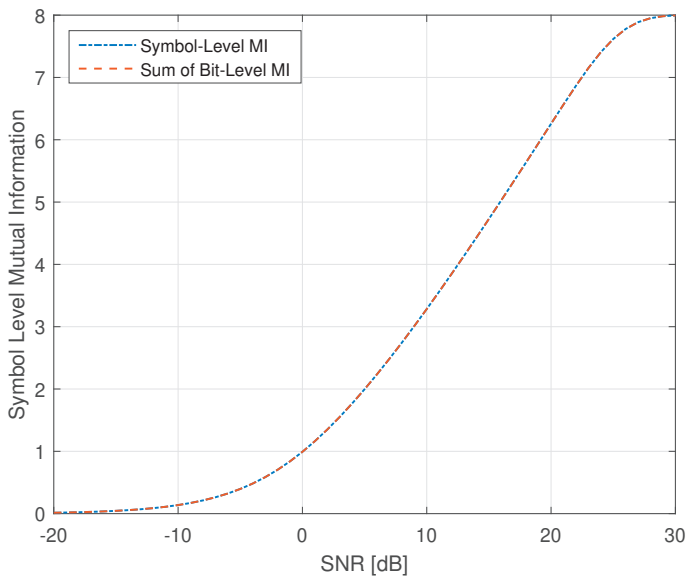

Figure 5.4: Illustration of compensating the minor loss in sum of RBIR for all bits using successive demodulation.

$$SI = \sum_{k=1}^{8} \Phi_k^{succ}. \tag{5.1}$$

The comparison of RBIR curves without employing successive demodulation Φ_k and with employing successive demodulation $\Phi_k^{(succ)}$ for 256-QAM is shown in Figure 5.3. It is verified that the sum of RBIR using successive demodulation, is equal to SI for 256-QAM as given by (5.1) and it is also illustrated in Figure 5.4. The idea of successive demodulation can also be extended to MLT where the information about successfully received codeword on most robust layer can be used to demodulate the codewords on less robust layers.

5.2.1 Performance of Successive Demodulation

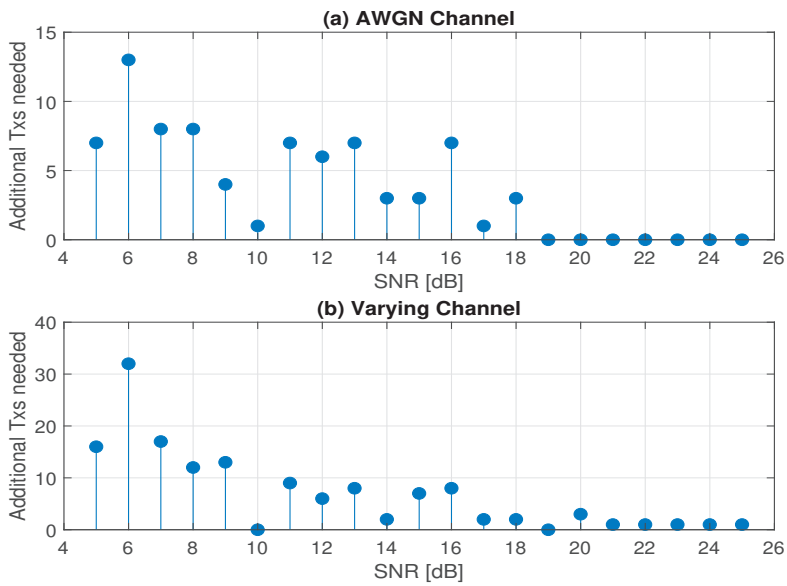

Figure 5.5: Performance of successive demodulation over (a) AWGN channel and (b) Varying channel.

The gain in adopting successive demodulation in MLT transmission is relatively small and thus the performance of successive demodulation is illustrated by determining the additional number of transmissions required in case of parallel demodulation with respect to successive demodulation. The simulation results for both AWGN channel and varying channel are shown in Figure 5.5, (a) and (b), respectively. During simulation, the successive demodulation technique is employed only when the codewords on robust layers are successfully received, otherwise the demodulation of codewords are done in parallel, thereby making no attempts to extract information from codewords on robust layers. It is seen in Figure 5.5 (a) and (b), that the additional number of transmissions needed is quite large at 6

dB as none of the layers will be successful over lower SNR range (i.e., SNR < 5 dB) and as soon as the SNR is around 6 dB, the codewords on the most robust layers will be successfully decoded, thus displaying the largest gain using successive demodulation on the respective channels. However, above 6 dB, the gain is still noticeable until 18 dB-20 dB but the gain drops to zero after 20 dB as the codewords on all layers have sufficient energy to be successfull in both the cases.

5.3 MLT with ARQ Scheme

The MLT technique can also be used with ARQ schemes by exploiting the layers of different robustness. Based on the end-user application, MLT with ARQ scheme can be employed in different ways. For instance, in case of real time applications (i.e. with low latency requirement), the packets related to such applications can be transmitted on the most robust layers such that the number of retransmissions required are considerably reduced, thereby reducing the delay in response.

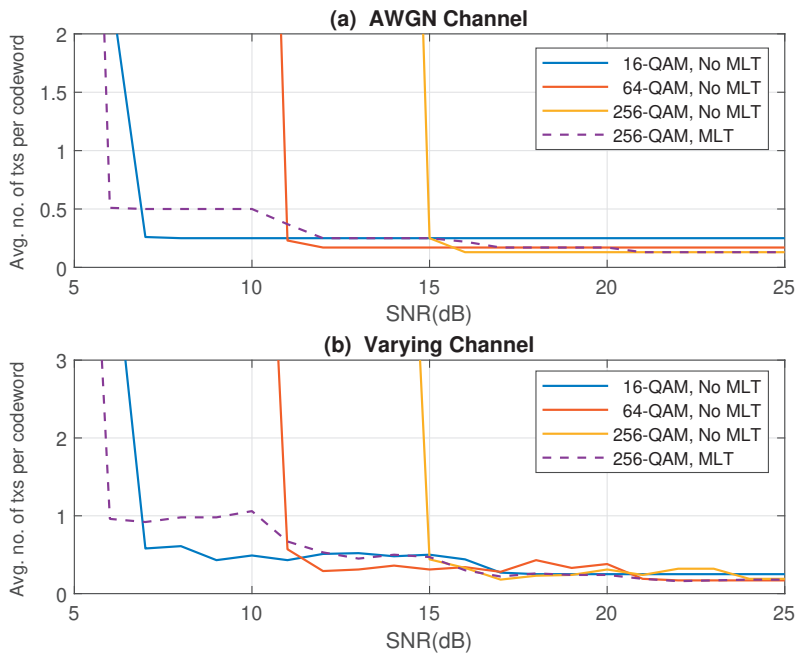

Figure 5.6: Performance of MLT Vs traditional approach using coded-ARQ scheme over (a) AWGN channel (b) Varying channel.

In order to appreciate the difference between MLT with basic ARQ scheme and traditional approach, the average number of transmissions needed per codeword to successfully decode 1000 codewords have been determined. Figure 5.6 (a) compares the performance of traditional approach using QAM of different modulation orders(i.e., M = 16, 64, 256) with the MLT using 256-QAM over AWGN channel. It is seen that until 6 dB, all the scenarios fail as they do not acquire sufficient

energy to successfully decode codewords. However, for SNR range from 6 dB to 7 dB MLT outperforms all the traditional approaches with different modulation order, as codewords on the first pair of robust layers are successfully decoded in case of MLT whereas the codewords transmitted using traditional approaches fail as they do not have sufficient received energy to succeed.

For SNR range from 7 dB to 10 dB, the traditional approach with 16-QAM performs better the MLT with 256-QAM as the codewords on layers corresponding to pair 2,3 and 4 fail in case of MLT whereas the codewords in case of traditional approach using 16-QAM succeed from 7 dB onward. However, MLT still provides better performance than traditional approach with 64-QAM and 256-QAM. For SNR range from 11 dB to 15 dB, codewords on the last two pairs(i.e., Pair 3 and Pair 4) of layers fail in case of MLT and the traditional approach using 64-QAM performs better than MLT as it has accumulated sufficient received energy above 11 dB.

For SNR range of 15 dB-21 dB, the average number of transmission per codeword drops for traditional approach using 256-QAM drops at 15 dB as it has received sufficient energy, on an average, to successfully decode codewords. However, the codewords on the least robust layers fail in case of MLT and thus, the traditional approach using 256-QAM has more gain in this region. The performance of MLT using 256-QAM coincides with that of traditional approach using 256-QAM for SNR above 21 dB as all the codewords on their respective layers succeeds. Thus, to summarize, MLT provides better performance than the traditional approaches with $M = 16, 64, 256$ for a given SNR range of interest. The very similar behavior is also observed in varying channel and it shown in Figure 5.6 (b).

Chapter 6
Conclusion and Future Work

6.1 Conclusion

In this thesis work, the theoretical study on MLT using the concepts of RBIR is described in detail and various simulation results are shown in order to illustrate the advantages of MLT and its variants. From simulation results, it was concluded that MLT outperforms traditional approach without the need for link adaptation technique especially when the channel is very unpredictable. Furthermore, the idea of mixing layers and successive demodulation techniques provided further gain in the performance of MLT. It was seen that the gain in employing successive demodulation was quite low however, the gain in mixing layers was more prominent, especially in the low SNR region. Lastly, it was concluded that the performance of MLT with ARQ scheme was noticeable when compared to traditional approach for a given SNR range of interest.

6.2 Future Work

The concepts of RBIR can be further exploited by looking at different code rates for a given SNR. Based on the applications like best effort services and real-time services, suitable code rates can be chosen over different layers. For instance, higher code rate can be used for transmitting the real-time service packets on the most robust layers and lower code rate for best-effort services on the least robust layers. Also, the performance of MLT can be further studied in combination with HARQ-IR scheme.

References

[1] C. E. Shannon, ”A Mathematical Theory of Communication,” The Bell System Technical Journal, pp. 379-423, Jul. 1948.

[2] A. Steiner and S. Shamai, "Multi-layer broadcasting hybrid-ARQ strategies for block fading channels," in IEEE Transactions on Wireless Communications, vol. 7, no. 7, pp. 2640-2650, July 2008.

[3] L. Wilhelmsson, S. Moloudi, and M. Lopez, ”Some results on HARQ performance in dense deployments”, doc.: IEEE 802.11/19/1133r0, available at https://mentor.ieee.org/802.11/dcn/19/11-19-1133-00-00be-someresults- on-harq-performance-in-dense-deployments.pptx

[4] C. Pettersson, L. Wilhelmsson, and M. Lopez, "Spectrum efficient transmission over unknown channels," Submitted to VTC-Fall 2020.

[5] R. G. Gallager, Information theory and reliable communication. John Wiley and Sons, 1968.

[6] W.E.Ryan and S.Lin, Channel Codes: Classical and Modern, Cambridge University Press, 2009.

[7] S. Gounai, T. Ohtsuki and T. Kaneko, "Modified Belief Propagation Decoding Algorithm for Low-Density Parity Check Code Based on Oscillation," 2006 IEEE 63rd Vehicular Technology Conference, Melbourne, Vic., 2006, pp. 1467-1471.

[8] Perahia, Eldad and Stacey, R.. (2008). Next generation wireless LANs: Throughput, robustness, and reliability in 802.11n.

[9] U. Wachsmann, R. F. H. Fischer and J. B. Huber, ”Multilevel codes: theoretical concepts and practical design rules”, IEEE Transactions on Information Theory, pp. 1361–1391, vol. 45, no. 5, July 1999

[10] L. Michael and D. Gómez-Barquero, "Bit-Interleaved Coded Modulation (BICM) for ATSC 3.0," in IEEE Transactions on Broadcasting, vol. 62, no. 1, pp. 181-188, March 2016.

[11] Shu Lin, D. J. Costello and M. J. Miller, "Automatic-repeat-request error-control schemes," in IEEE Communications Magazine, vol. 22, no. 12, pp. 5-17, December 1984.

[12] IEEE 802.16m-08/004r5, "IEEE 802.16m Evaluation Methodology Document," Jan. 2009; http://ieee802.org/16/tgm/index.html

Appendix A

Appendix

A.1 Constellation Diagrams

A.1.1 Gray Mapping for 4-QAM

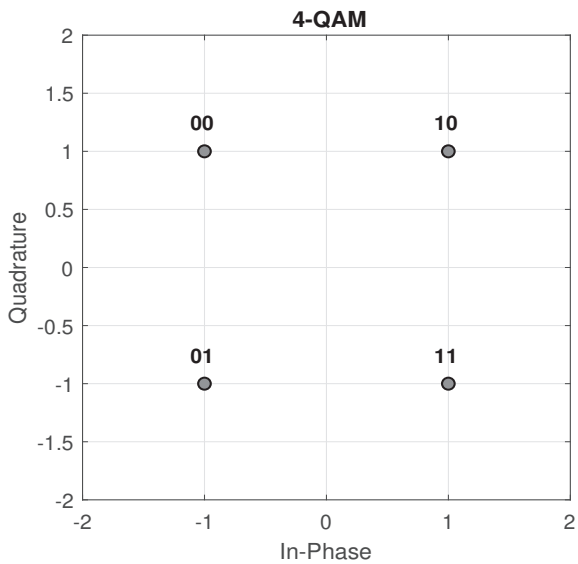

A.1.2 Gray Mapping for 16-QAM

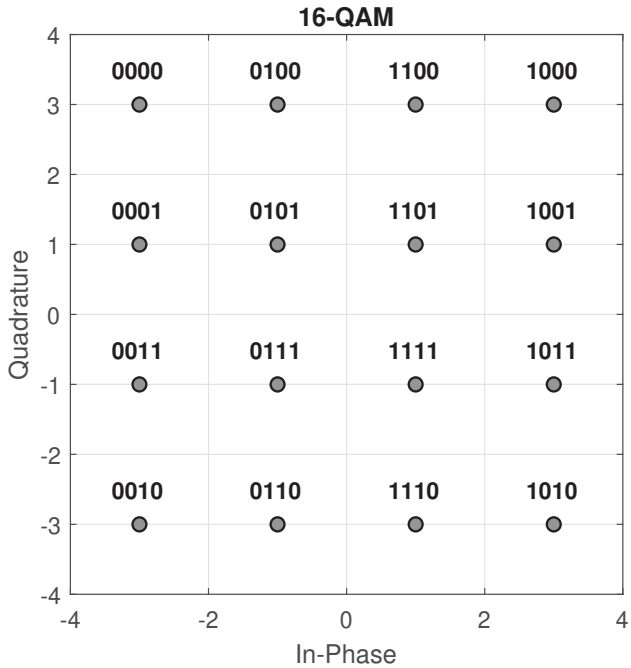

A.1.3 Gray Mapping for 64-QAM

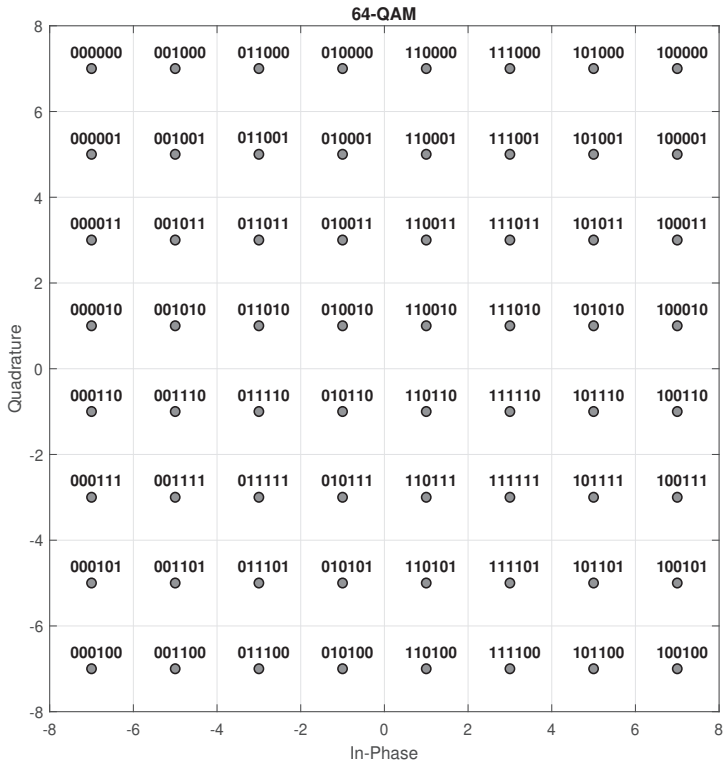

A.1.4 Gray Mapping for 256-QAM

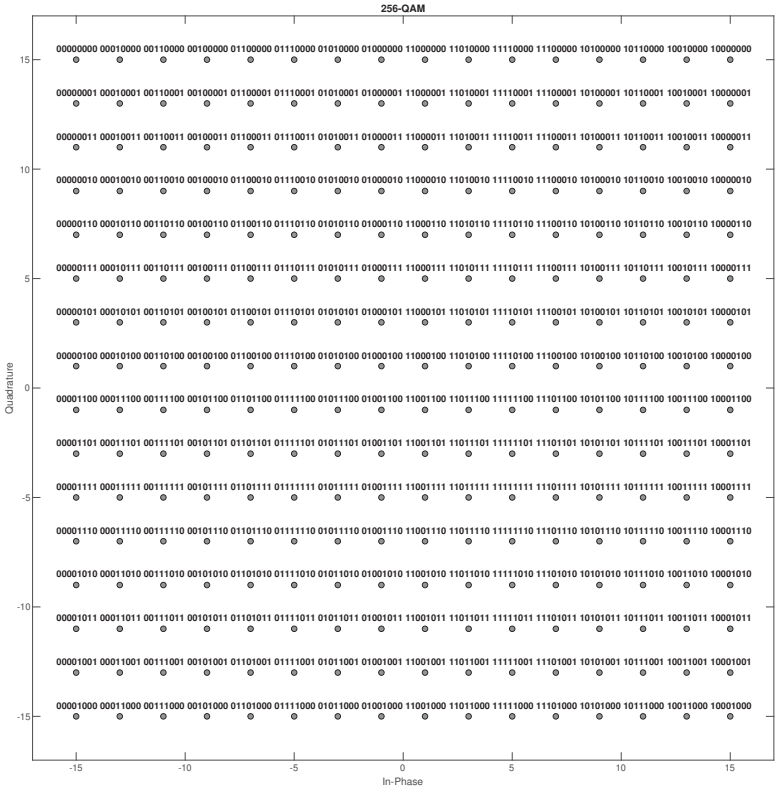

Printed by Tryckeriet i E-huset, Lund 2020

LUND
UNIVERSITY

Series of Master's theses
Department of Electrical and Information Technology
LU/LTH-EIT 2020-763
http://www.eit.lth.se